

AN INVESTIGATION OF SCENE-REFERRED COLOR SPACE BASED ON IMAGE CAPTURE OF REAL OBJECTS WITH A HIGH COLOR-FIDELITY DIGITAL CAMERA SYSTEM

Yasuharu Iwaki*, Masayuki Kuramoto*, Hitoshi Urabe* and Hiroaki Sugiura**
 *Fuji Photo Film Co., Ltd, Equipment R&D Center; Japan.
 **Mitsubishi Electric Corporation, Advanced Technology R&D Center; Japan.

Abstract

A camera system capable of acquiring colorimetric images of a scene has been developed. By using the system, the color reproduction gamuts for scenes each containing highly color-saturated reflective objects, fluorescent objects, or semi-transparent objects were measured.

It was confirmed that the fluorescent objects scene and the semi-transparent objects scene have color reproduction gamuts exceeding that of optimal color[1], and we considered the method of dealing with scene data exceeding optimal color.

Introduction

Trials of an image processing workflow starting with a scene image have recently commenced. ISO 22028-1[2] defines the concept of 'Image State' and describes an image processing workflow from Scene Referred Image to Output Referred Image. Windows Vista TM[3] of Microsoft provides support for a color workflow capable of maintaining a wide gamut for color reproduction using sRGB[4] for scene space description.

In the present paper, using a camera system consisting of a black-and-white CCD digital camera and a set of three optical filters approximating the color matching functions, and thus capable of high fidelity scene capture, the colour of a range of different types of object (reflective, fluorescent and semi-transparent) was measured, and the range of color needed to describe practical scenes was calculated.

By clarifying the range for actual scene color, expansion to a variety of applications including the establishment of a standard describing the color space for real scenes, spectral sensitivity design of a DSC for scene colorimetry, study of image conversion from a scene referred image to an output referred image is expected.

Camera System

The present system comprises a monochromatic digital camera (modified FinePix S2 Pro), a lens (Nikon AF Zoom, Nikkor ED 28-200 mm, F3.5-5.6G), three vapor-deposited color filters, a rotation-regulating controller (fabricated in-house) and a PC (Figure 1).

The image-shooting operation and camera settings (shutter speed and aperture) are controlled by the PC.

The captured image size is 13 M pixels for each channel (after honeycomb interpolation).

The characteristics of the color filters are shown Figure 2. $\bar{x}(\lambda), \bar{y}(\lambda), \bar{z}(\lambda)$ are the results of linear approximation of the color filters to $\bar{x}(\lambda), \bar{y}(\lambda), \bar{z}(\lambda)$. The calculated Q-Factor values for the three filters are R = 0.999, G = 0.992, B = 0.983, respectively.

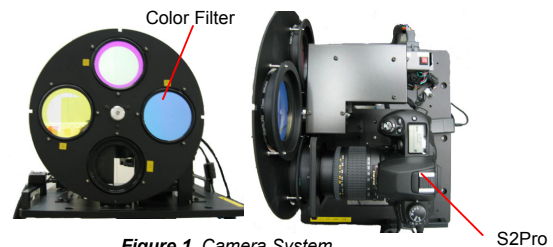


Figure 1. Camera System.

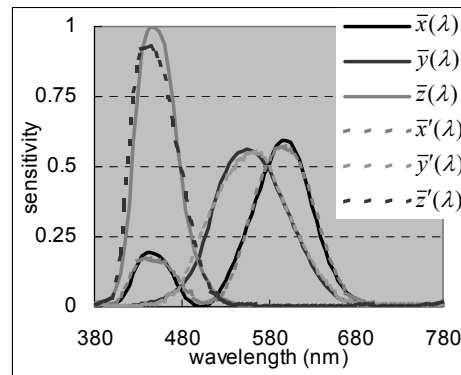


Figure 2. CIE color-matching functions $\bar{x}(\lambda)$, $\bar{y}(\lambda)$, $\bar{z}(\lambda)$, (2 degrees) and $\bar{x}'(\lambda)$, $\bar{y}'(\lambda)$, $\bar{z}'(\lambda)$.

Method of forming colorimetric scene images

The method of forming colorimetric scene image data (x, y and z images) from the captured images will be described. The processing flowchart is shown in Figure 3.

Prior to scene shooting, color charts and a white plate are shot under the same lighting condition as in scene shooting. In the present experiment, a Macbeth Color Checker and an NCS (Neutral Color System) chart were used. Figure 4(a) shows the actual scene containing the color charts. The color charts and the white plate are measured also with a spectral radiometer CS-1000 (a product of Konica-Minolta).

Since shooting is sequentially performed along with the rotation of the three filters, there arise certain fluctuations due to the variation in camera shutter operation, etc. Moreover, there

exist slight spectral discrepancies between the spectral characteristics of the camera and the color-matching functions.

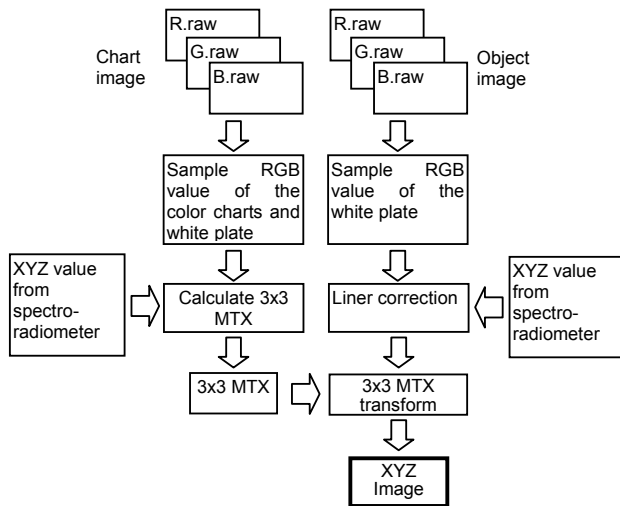


Figure 3. Flow chart to acquire the scene XYZ image.



Figure 4. Color Charts for calibration (a) and an example of reflective objects scene (b).

To correct these error sources, a 3x3 matrix for the conversion from RGB to XYZ is calculated based on least square approximation among the values measured with the aforementioned spectral radiometer, the characteristic values of the white plate and the color charts in the three scenes.

Next, each scene is captured by rotating the three filters. As is shown in Figure 4(b), the white plate is arranged in each scene, and its characteristics measured with the spectral radiometer.

The R, G and B values in the three images are linearly corrected in such a manner that the X_w , Y_w and Z_w values calculated by the aforementioned 3x3 Matrix match the X'_w , Y'_w and Z'_w values obtained by the measurement with the spectral radiometer on the basis of the average R, G and B values of the white plate portion of the three images.

Finally, by applying the 3x3 Matrix to the entire image, an XYZ image is obtained.

The colorimetric accuracy of the present colorimetric camera system confirmed by the above-described procedure is shown in Figure 5.

Table 1. Evaluation of our camera system with respect to colorimetric accuracy. Evaluated charts are macbeth color checker and NCS chart which are shown in Figure 4.

delta-E average of 64 patches	delta-E average of 6 gray patches	delta-E maximum
1.86	0.54	6.25

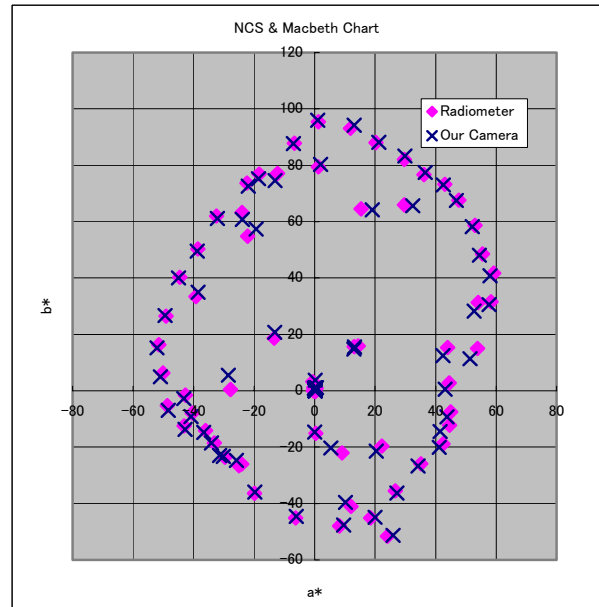


Figure 5. Evaluation of our camera system with respect to colorimetric

Shooting conditions

Figure 6 illustrates the arrangements for scene shooting.

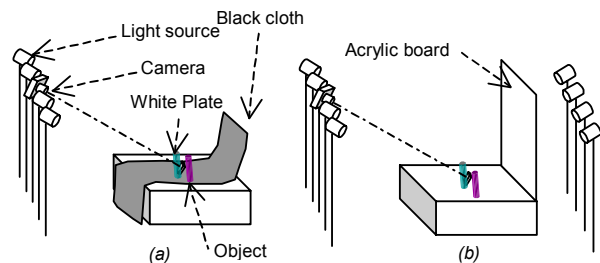


Figure 6. Lighting conditions. Set (a) is for reflective objects scenes and fluorescent objects scenes. Set (b) is for semi-transparent objects

The light source was Artificial Sunlight XC-500AF made by Seric(Figure 7). For shooting reflective objects, four lights were used arranged at the same height and distance as those of the camera. Semi-transparent objects were arranged in front of a milky white, diffuse acrylic board, and irradiated with four lights arranged in the rear of the acrylic board. For shooting fluorescent objects, the standard filters placed in front of the light source were replaced by those that were specially designed so as not to cut UV light.

The shooting conditions including lighting condition were entrusted to a professional photographer, who realized flat lighting with uniform intensity along the horizontal direction throughout the scene whereby the objects to be recorded were uniformly illuminated.

The position of the camera was set perpendicular to the plane of the white plate, whose setting angle had been finely adjusted so as to give the maximum luminance to the camera direction.

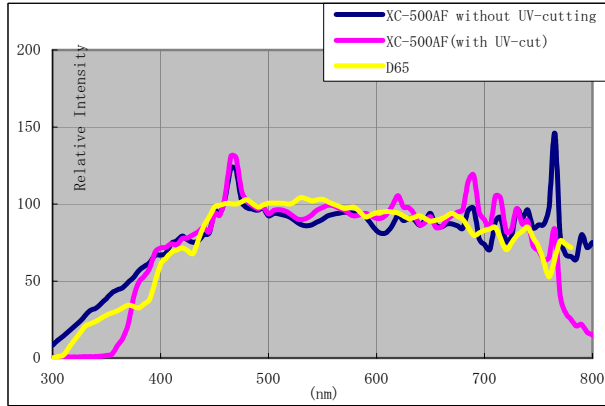


Figure 7. Spectra of the light sources.

Reflective objects

The scenes to be captured are shown in Figure 8.

In advance of the final experiment, preliminary experiments were repeated twice. Based on the information of the preliminary experiments, shooting objects with color saturations as high as possible were chosen.

In the preliminary experiments, objects such as flowers, etc. of natural origin were tested. Such objects proved to be not so highly saturated and were excluded from the final shooting. They were also excluded because of the difficulty in consistent reproduction.



Figure 8. Reflective objects scenes.

Calculation of Scene-referred color gamut

The calculation flow for scene color gamut starting with the captured image is shown in Figure 9.

From the captured XYZ images, edge-extracted images are formed that are used to avoid the effect of false colors. For edge extraction operation, the Sobel operator is used [5], and edge expansion operation is further carried out. XYZ values averaged by a 5x5 mask are calculated for the pixels except those in the edge portions, and converted to CIE1976L*C*H*. Then, for each region with an L* interval of 5 and an H* interval of 10 degrees, the loop calculation for obtaining the maximum of C* is repeated on all the pixels.

In this way the color gamut of each captured image was calculated.

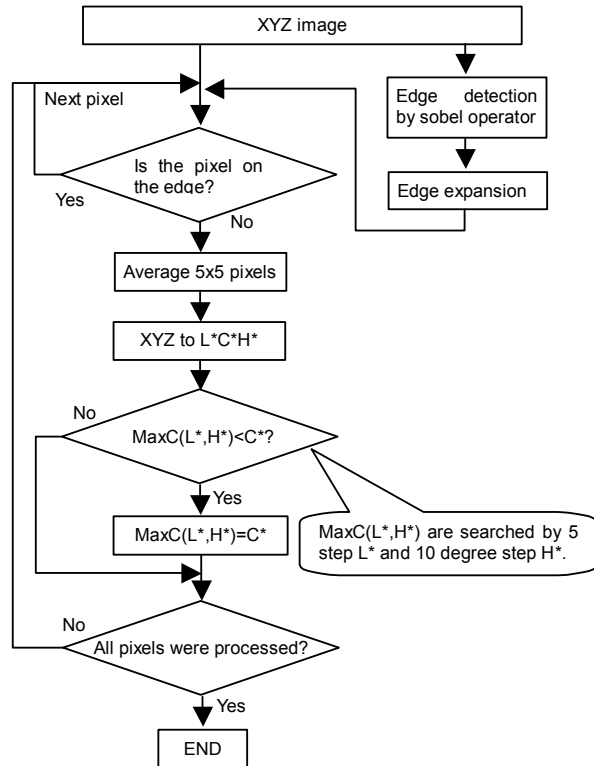


Figure 9. Flow chart to calculate scene color gamut.

Gamut of reflective objects scenes

The results of the gamut calculation for reflective objects scenes are shown in Figure 10.

The Optimal Color is the locus of the most saturated colors obtained by the CIE1931 Standard color observer ($\bar{x}(\lambda), \bar{y}(\lambda), \bar{z}(\lambda)$). All the gamuts calculated from the actual scenes, and those of AdobeRGB and Pointer were converted to those under D50 light source according to the VonKries rule[6]. The color hue angles for the C*-L* plot represent the cross-sections of R-C, G-M and B-Y with reference to the primaries of AdobeRGB. The gamut for the reflective objects scenes exceeds those of AdobeRGB and Pointer's real surface color [7]. In particular, it is seen that the Cyan and Blue regions are larger towards the low luminance side.

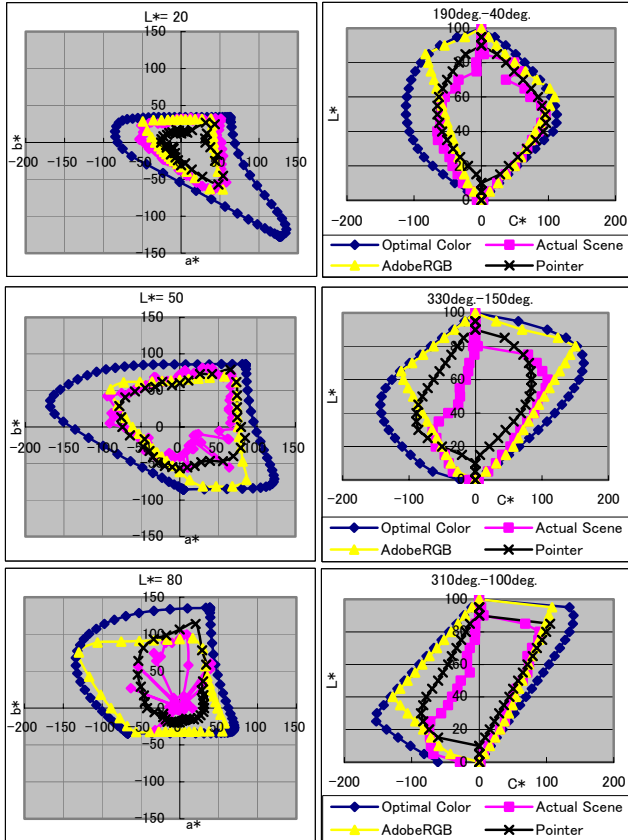


Figure 10. Scene gamut plots for reflective object scene. The left side shows a^*b^* cross section at $L^*=20, 50$ and 80 . The right side shows an example of C^*L^* cross section at primary and secondary colors.

Gamut of fluorescent objects scenes

In Figure 11, the fluorescent objects scenes are shown. Figure 12 shows the gamut calculated from these fluorescent objects scenes. It is evident that the gamut exceeds that of Optimal Color particularly towards the high luminance side.

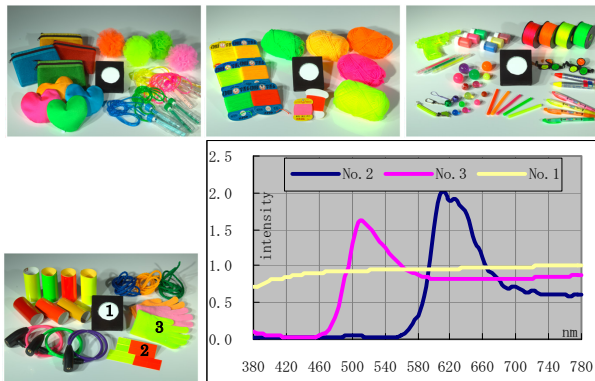


Figure 11. Fluorescent objects scenes and spectrum from fluorescent object. Calculated values (L^*, a^*, b^*) from the spectrum are (73.6, 89.1, 95.9) at No. 2 and (101.6, -50.8, 166.3) at No. 3.

In Figure 11, the spectra of two objects measured with the spectral radiometer are shown together with that of the white plate. It is seen that in specific wavelength regions, the reflectance exceeds 1.0 due to excitation radiation phenomenon. It is also seen that the L^* , a^* and b^* values calculated from these spectra exceed those of Optimal Color with L^* values larger than 100.

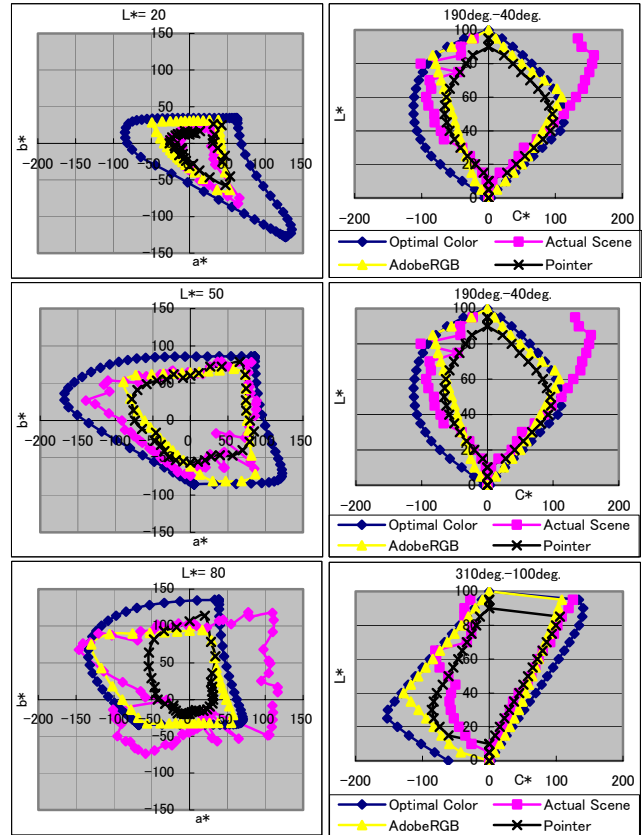


Figure 12. Scene gamut plots for fluorescent object scene. The left side shows a^*b^* cross section $L^*=20, 50$ and 80 . The right side shows an example of C^*L^* cross section at primary and secondary colors.

Gamut of semi-transmissive objects scenes

In Figure 13, the semi-transmissive objects scenes are shown, and the gamut calculated from these semi-transmissive objects scenes is shown in Figure 14. Also in the semi-transmissive objects scenes, it is evident that the gamut exceeds that of Optimal Color at the high luminance region. In addition, the gamut region expands more towards the high luminance direction.

Figure 13 shows the spectra of three objects measured with the spectral radiometer. It is evident that the reflectance exceeds 1.0 since light more intense than that from the white plate is emitted from the semi-transmissive object due to lighting from behind the scene.

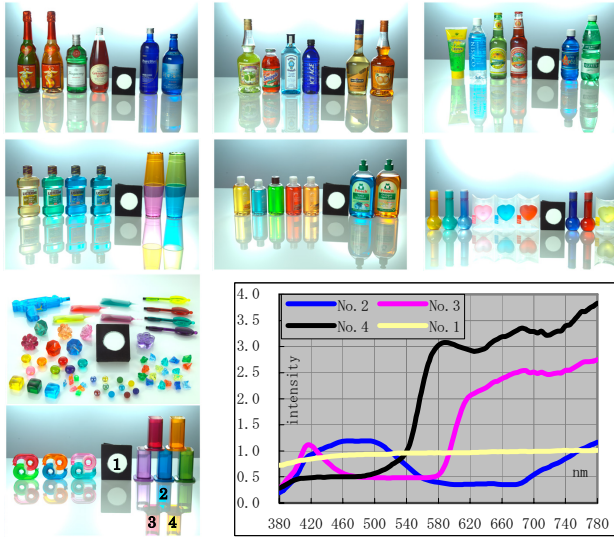


Figure 13. Semi-transmissive objects and spectrum from semi-transmissive object.
 Calculated values (L^*, a^*, b^*) from the spectrum are (77.7, 38.1, -8.6) at No. 2, (91.3, 65.2, 8.2) at No. 3 and (128.8, 42.1, 89.9) at No. 4.

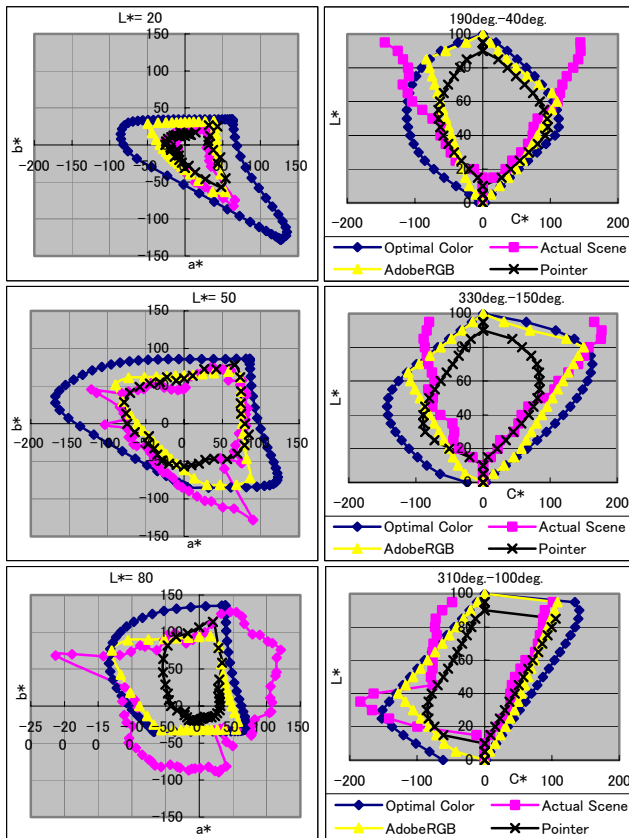


Figure 14. Scene gamut plots for semi-transmissive object scene. The left side shows a^*b^* cross section at section $L^*=20, 50$ and 80 . The right side shows an example of C^*L^* cross section at primary and secondary colors.

Discussion

The scene gamut for the reflective objects scenes is wide at low luminance. Since the angle of the white plate was adjusted so that the plate appears the brightest, the reflected light included a specular component. This situation is different from the ordinary geometric colorimetric condition [8] ($45^\circ X$) and different from the geometric condition for reflective object. For these reasons, the luminance of the reflective object may look relatively dark.

In the case of fluorescent objects, the reflectance exceeds 1.0 at some wavelengths due to the fluorescence excitation phenomenon. According to the CIELAB representation, wherein the adaptation light source is defined based on the white plate, the L^* value inevitably has a value exceeding 100, and therefore the gamut exceeds that of Optimal color.

Since semi-transmissive objects are also brighter than the white plate, the situation is similar. Hence, in dealing with actual scene images containing a fluorescent or semi-transmissive object, the definition of the light source white as the reference is a significant problem.

In the future, the following research targets will be studied.

- Object color in the region exceeding $L^* = 100$, i.e., $Y = 100$ with respect to the fluorescent and semi-transparent scenes, which was not calculated in the present paper, will be included.
- Development of the evaluation method for the spectral sensitivities of a colorimetric DSC.
- Study of image conversion from scene referred images to output referred images.

Acknowledgement

This research was organized in part by the New Energy and Industrial Technology Development Organization, Japan (NEDO).

References

- [1] R.W.G.Hunt, "The reproduction of colour (6th edition)", New York: John Wiley & Sons Inc., (2004), pg.88.
- [2] ISO 22028-1, "Photography and graphic technology- Extended colour encodings for digital image storage, manipulation and interchange- Part 1: Architecture and requirements", (2004).
- [3] Microsoft Corporation, "Windows Color System: The Next Generation Color Management System- White Paper", (2005), <http://www.microsoft.com/whdc/device/display/color/WCS.msp>.
- [4] IEC 61966-2-2, "Multimedia systems and equipment- Color measurement and management- Part 2-2: Color management- Extended RGB colour space- sRGB", (2003).
- [5] R. O. Duda and P.E. Hart, "Pattern Classification and Scene Analysis", New York: John Wiley & Sons Inc., (1971), pg. 267-272.
- [6] J.von kries, "Chromatic adaptation", Festschrift der Albrecht-Ludwig-Universitat(Fribourg), (1902).
- [7] Pointer, Michael, R, "The gamut of real surface colors", Color Research & Application 5, (1980), pp. 145-155.
- [8] CIE15:2004, "Colorimetry", 3rd Edition (2004).

Author Biography

Yasuharu Iwaki received his MME degree in electronics and information engineering from Nagaoka University of Technology in 1993. From 1993 he is working for Fuji Photo Film Co., Ltd.. His work has focused on the development of digital imaging for photographic printer.